Audio Engineering Society

Conference Paper

Presented at the AES 2026 International Conference on
Audio for Virtual and Augmented Reality and Immersive Games
2026 June 30 – July 3, Paris, France

*This conference paper was selected based on a submitted abstract and 750-word precis that have been peer reviewed by at least two qualified anonymous reviewers. The complete manuscript was not peer reviewed. This conference paper has been reproduced from the author's advance manuscript without editing, corrections, or consideration by the Review Board. The AES takes no responsibility for the contents. This paper is available in the AES E-Library (http://www.aes.org/e-lib), all rights reserved. Reproduction of this paper, or any portion thereof, is not permitted without direct permission from the Journal of the Audio Engineering Society.*

# A framework for 6DoF 4pi reverberation generation using wave-based-derived virtual sound sources.

Ryoko Hara[1], Masataka Nakahara[2,1], and Akira Omoto[3,2]

[1]*SONA Corporation, Tokyo 164-0013 Japan*
[2]*ONFUTURE Ltd, Tokyo 141-0032 Japan*
[3]*Kyushu University, Fukuoka 815-8540 Japan*

Correspondence should be addressed to Ryoko Hara (hara@sona.co.jp)

**ABSTRACT**

Realistic reproduction of spatial reverberation is essential for immersive audio applications, including virtual reality and interactive gaming. While geometrical acoustics methods enable efficient rendering, they do not fully capture wave phenomena. Wave-based simulations provide higher physical accuracy but at substantial computational cost. This paper extends VSVerb, a 4pi sampling reverberator based on virtual sound sources (VS) extracted via sound intensity analysis, to use pressure and three-axis particle velocity computed by a discontinuous Galerkin finite element method (dG-FEM) simulation, enabling reverberation that reflects the wave-based acoustic characteristics of virtual spaces to be generated. Experiments in a university lecture room show that the proposed method produces room acoustic parameters closer to those of the measured impulse response than geometrical acoustics ray tracing across most metrics and frequency bands. Furthermore, the VS distribution from a single simulation is adapted to different receiver positions by updating the geometric contribution of each VS. Receiver position adaptation for 6DoF navigation is also demonstrated from a single simulation, maintaining the advantage over geometrical acoustics at all evaluated positions. These results indicate the potential of the proposed framework for wave-based interactive reverberation in virtual spaces.

## 1 Introduction

Realistic reproduction of spatial reverberation is a fundamental requirement for immersive audio in virtual reality, augmented reality, and interactive gaming. Geometrical acoustics (GA) methods, such as the image source method and ray tracing, are widely used for their computational efficiency, but do not fully capture wave phenomena such as diffraction and low-frequency modal behavior. In contrast, wave-based methods, including finite-difference time-domain (FDTD), finite element methods (FEM), and boundary element methods (BEM), provide higher physical accuracy at the cost of substantial computational resources.

The virtual sound source (VS) framework represents the reverberant field as a set of discrete sources characterized by direction of arrival, arrival time, and energy.

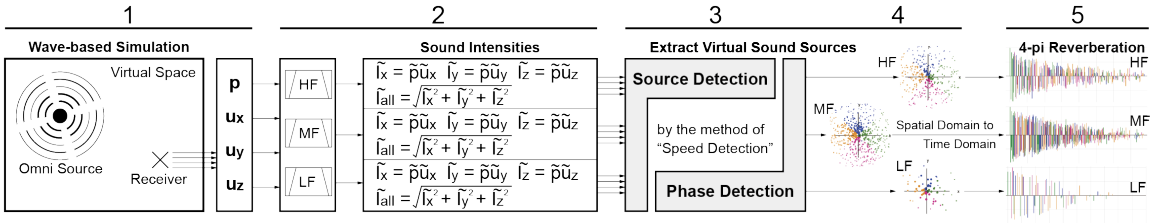



**Fig. 1:** Overview of the proposed framework.

Foundational work on sound-intensity-based source extraction [1–3] established the basis for this approach. The authors have developed VSVerb, a 4pi sampling reverberator that generates reverberation from VS distributions extracted via sound intensity analysis of measured pressure and three-axis particle velocity [4]. VSVerb has been applied practically as a reverb plugin for archiving the acoustics of a recording studio, demonstrating its suitability for professional audio production workflows [5].

A natural extension of VSVerb is the generation of reverberation for virtual spaces that do not physically exist—a key application in virtual reality and immersive audio. By supplying VSVerb with pressure and three-axis particle velocity computed by a wave-based simulation, the physical accuracy of wave-based methods can be incorporated into the VS-based reverberation framework. This paper investigates whether simulation-derived inputs can produce equally valid VS distributions as measured inputs, and whether the resulting reverberation is suitable for virtual spaces. A preliminary study using FDTD-derived inputs was reported [6]; the present work employs the discontinuous Galerkin finite element method (dG-FEM), which offers higher computational efficiency.

## 2 Proposed Framework

### 2.1 Virtual Sound Source Extraction

The VS extraction pipeline takes as input pressure $p(t)$ and three-axis particle velocity $u_x(t)$, $u_y(t)$, $u_z(t)$ computed by the dG-FEM simulation at a receiver position. The overall framework is illustrated in Fig. 1. The processing is performed independently in three frequency bands—low (LF: 90–500 Hz), mid (MF: 200–3000 Hz), and high (HF: 1000–8000 Hz)—to account for frequency-dependent acoustic behavior. In each band, three-axis active sound intensities $I_x$, $I_y$, $I_z$ are computed from $p$ and $(u_x, u_y, u_z)$ [7], and virtual sound sources are extracted using the Speed Detection method [8]. This method distinguishes coherent reflection components (Source Intensities) from incoherent residual components (Drifting Intensities) based on the spatial moving speed $v(t)$ of the instantaneous intensity vector.

In the present work, the improved adaptive thresholding scheme [9] is employed. The adaptive threshold $v_t(t)$ is derived from the local statistics of $v(t)$:

$$v_t(t) = \frac{1}{T(t)} \int_{t-T(t)/2}^{t+T(t)/2} v(\tau)\, d\tau$$

where $T(t)$ is a time-varying window. Source Intensities are detected at time indices $t_s$ satisfying $\bar{v}(t_s) \leq v_t(t_s)$, where $\bar{v}(t)$ is a short-term smoothed estimate of $v(t)$.

Each detected Source Intensity segment $k$ yields a VS characterized by its arrival time $\tau_k$, direction of arrival $\hat{\mathbf{d}}_k$ (unit vector), and amplitude $I_k$. The phase polarity ($\pm$) of each VS is estimated from the pressure waveform using the Phase Detection method [9]. The complete VS distribution of $K$ detected sources is denoted $\mathscr{V} = \{(\hat{\mathbf{d}}_k, \tau_k, I_k, \phi_k)\}_{k=1}^{K}$.

### 2.2 Virtual Room Impulse Response Synthesis

The VS distribution is used to synthesize a 4pi directional room impulse response. Because every reflection carries explicit directional information, the VS distribution can be divided into any target playback channel format by assigning each VS to the appropriate channel according to its arrival direction. The resulting channel signals can be applied to any playback format—from stereo and binaural to multichannel loudspeaker systems—making VSVerb adaptable to a wide range of spatial audio applications [4].

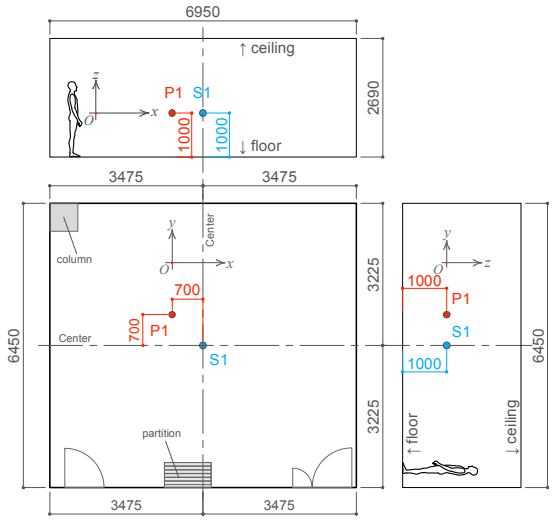



**Fig. 2:** Plan and cross-sectional view of source position S1 and receiver position P1.

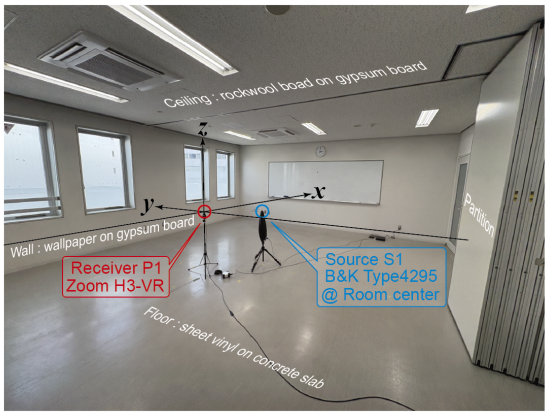



**Fig. 3:** Lecture room, loudspeaker and A-format microphone for the measurements.

**Table 1:** Number of detected VS at P1.

| Freq. band | M-VS | S-VS |
|---|---|---|
| HF | 706 | 617 |
| MF | 713 | 689 |
| LF | 444 | 612 |

## 3 Experimental Setup

### 3.1 Acoustic Environment

Experiments to validate the proposed method were conducted in a lecture room at Tokyo University of the Arts, Tokyo, Japan. The room has plan dimensions of approximately 6.95 m × 6.45 m and a ceiling height of 2.69 m, yielding a volume of approximately 117.8 $m^3$. The room was unoccupied, with chairs and desks removed. Surface finish materials were: floor—sheet vinyl on concrete slab; ceiling—rockwool board on gypsum board; walls—wallpaper on gypsum board.

### 3.2 Measurement Setup

A single omnidirectional sound source (B&K Type 4295) was placed at source position S1 at the center of the room at a height of 1.0 m above floor level. Acoustic measurements were performed at receiver position P1 at the same height, using a Zoom H3-VR A-format microphone. P1 has lateral and longitudinal offsets of $(0.7, 0.7)$ m from S1 in the horizontal plane. The source–receiver layout is shown in Fig. 2, and the measurement equipment is shown in Fig. 3.

Room impulse responses were acquired using a log swept-sine signal. The A-format microphone signals were converted to pressure $p(t)$ and three-axis particle velocity $(u_x(t), u_y(t), u_z(t))$ via simple linear combinations of the capsule outputs [10], from which sound intensities were computed and the VS extraction pipeline was applied.

### 3.3 Wave-Based Acoustic Simulation

Wave-based simulations were performed using COMSOL Multiphysics with dG-FEM in the time-explicit formulation. The simulation domain approximated the room geometry as a rectangular enclosure with two geometric modifications: removal of a structural column in the lower-left corner and a movable partition in the center-right region. Frequency-dependent absorption coefficients were assigned to the ceiling at octave-band center frequencies of (63, 125, 250, 500, 1k, 2k) Hz with values of (0.23, 0.33, 0.45, 0.68, 0.71, 0.82), respectively. Constant absorption coefficients of 0.10 and 0.03 were applied to the walls and floor, respectively. The simulation was computed up to a maximum frequency of 2 kHz with a duration of 0.5 s. The source was placed at S1 and pressure and particle velocity were recorded at P1.

### 3.4 Results

Table 1 shows the number of VS detected in each frequency band for the measurement-based (M-VS) and

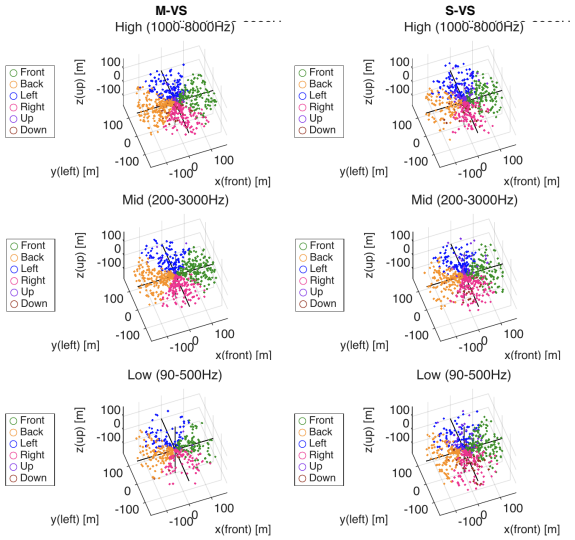



**Fig. 4:** VS distributions at P1: M-VS and S-VS.

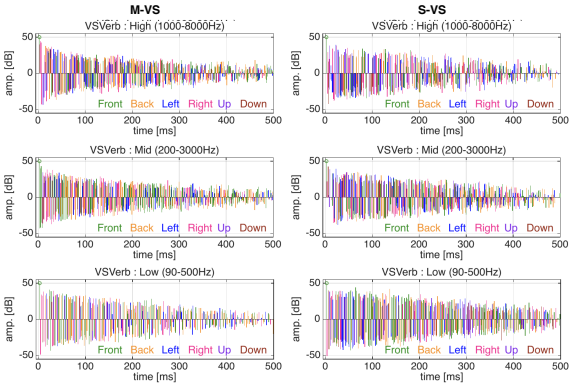



**Fig. 5:** VSVerb at P1: M-VS and S-VS.

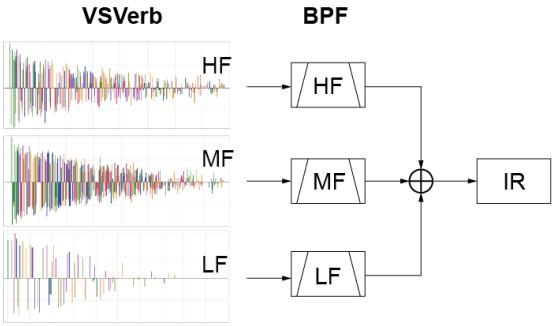



**Fig. 6:** Processing pipeline for deriving an impulse response from the VSVerb output for room acoustic parameter evaluation.

simulation-based (S-VS) conditions at P1.

Fig. 4 shows the VS distributions and Fig. 5 shows the corresponding VSVerb in time domain. Colors in Figs. 4 and 5 indicate the direction of arrival of each VS. The spatial patterns of M-VS and S-VS show overall similarity across frequency bands. The overall temporal envelopes are also comparable, indicating that the simulation-derived VS pipeline reproduces the reverberant structure of the measured data.

## 4 Evaluation

A key motivation for this work is to explore the possibility of using VSVerb to generate reverberation for virtual acoustic spaces that sounds as realistic as that of real environments. To examine this, the following four conditions are compared at receiver position P1:

- **M-IR**: measured omnidirectional IR; reference.
- **M-VS**: measurement-based VS — acoustic measurement → VS extraction → virtual IR.
- **S-VS** (proposed): dG-FEM at P1 → VS extraction → virtual IR.
- **GA-IR**: COMSOL ray tracing (100,000 rays, 0.5 s) at P1; same absorption coefficients as the dG-FEM simulation.

M-IR serves as the reference representing the real acoustic environment. M-VS is included to characterize the inherent properties of the VSVerb pipeline when applied to measured data. GA-IR is included as a representative geometrical-acoustics-based method widely used in interactive audio applications.

VSVerb is converted to an impulse response, and room acoustic parameters are computed for quantitative comparison. Specifically, since VSVerb holds time and level information for each VS independently in each frequency band, an impulse response is obtained by applying a corresponding bandpass filter to each VS and summing the contributions across all VS and bands. This processing pipeline is illustrated in Fig. 6.

Table 2 shows T20, C80, D50, and Ts for M-IR, S-VS, and GA-IR, computed over the same LF, MF, and HF

bands used for VS extraction, together with the overall average (All). The diff. rows indicate the deviation from M-IR; bold values indicate the smaller absolute deviation. S-VS shows smaller deviations from M-IR than GA-IR across almost all metrics and frequency bands.

Fig. 7 shows T20, C80, D50, and Ts per octave band for all four conditions, with JND error bars (ISO 3382-1 [11]) as a perceptual reference. The values are computed over the same LF, MF, and HF bands as VS extraction, and the overall average (All). M-VS and S-VS show close agreement across most frequency bands, confirming that dG-FEM-derived inputs produce VS distributions equivalent to those from measured data.

A common trend observed in both Table 2 and Fig. 7 is that S-VS tends to underestimate T20 relative to M-IR, resulting in a drier, less reverberant sound. For the other metrics, S-VS shows favorable agreement with M-IR.

**Table 2:** Room acoustic parameters at P1: M-IR (reference), S-VS, and GA-IR.

| Metric (JND) | Cond. | Freq. band | | | |
|---|---|---|---|---|---|
| | | LF | MF | HF | All |
| T20 (±5%) | M-IR | 0.90 | 1.31 | 1.37 | 1.29 |
| | S-VS | 1.09 | 1.08 | 1.06 | 1.06 |
| | diff. | +21.3% | **−17.4%** | **−22.2%** | **−17.6%** |
| | GA-IR | 0.84 | 0.87 | 0.85 | 0.86 |
| | diff. | **−6.2%** | −33.3% | −37.6% | −33.5% |
| C80 (±1.0 dB) | M-IR | 8.0 | 8.6 | 9.2 | 9.0 |
| | S-VS | 4.8 | 6.7 | 6.2 | 6.2 |
| | diff. | **−3.2** | **−1.9** | **−3.0** | **−2.8** |
| | GA-IR | 15.8 | 15.5 | 13.4 | 13.7 |
| | diff. | +7.9 | +6.9 | +4.2 | +4.7 |
| D50 (±0.05) | M-IR | 0.744 | 0.823 | 0.848 | 0.832 |
| | S-VS | 0.588 | 0.739 | 0.719 | 0.718 |
| | diff. | **−0.155** | **−0.084** | −0.129 | −0.114 |
| | GA-IR | 0.954 | 0.954 | 0.928 | 0.932 |
| | diff. | +0.210 | +0.131 | **+0.080** | **+0.100** |
| Ts (±10.0 ms) | M-IR | 38.2 | 32.5 | 29.2 | 30.6 |
| | S-VS | 57.9 | 39.2 | 43.1 | 43.1 |
| | diff. | **+19.7** | **+6.6** | **+13.9** | **+12.5** |
| | GA-IR | 9.1 | 8.7 | 14.0 | 13.1 |
| | diff. | −29.1 | −23.9 | −15.3 | −17.5 |

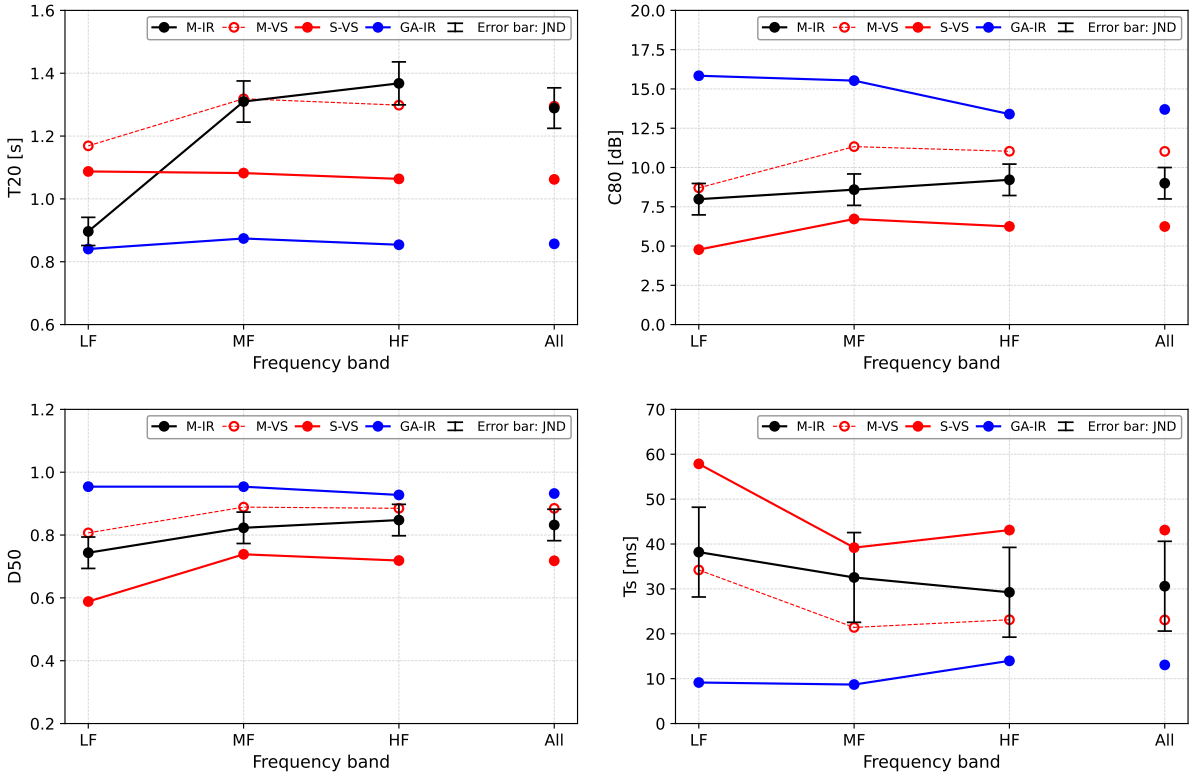



**Fig. 7:** Room acoustic parameters at P1: T20, C80, D50, and Ts for M-IR, M-VS, S-VS, and GA-IR. Error bars indicate JND.

It should be noted that both M-VS and S-VS differ from M-IR, which is a characteristic of VS-based reverberation. While a conventional IR-based convolution reverb directly convolves a source signal with the full measured impulse response, VSVerb instead extracts individual VS from the sound intensity response and synthesizes reverberation from them independently for each frequency band. This renders each reflection with its own spatial direction, allowing flexible control of directionality and level balance across bands, but also results in a generated IR that differs structurally from the directly measured M-IR. The close similarity between M-VS and S-VS confirms that this difference is inherent to the VSVerb pipeline rather than a result of simulation inaccuracy. Nevertheless, S-VS shows smaller deviations from M-IR than GA-IR across many frequency bands and metrics, demonstrating the advantage of wave-based simulation input for virtual space reverberation.

## 5 Discussion

A key challenge observed in the results is that S-VS tends to underestimate T20, producing a drier sound than M-IR. Notably, the T20 derived from the dG-FEM pressure impulse response alone showed a similar tendency, suggesting that this issue is related to simulation accuracy rather than the VSVerb pipeline itself, and may be improved through more precise simulation modeling. For example, the room geometry is currently approximated as a rectangular enclosure with only two geometric modifications, and scattering from irregular boundaries is not fully represented. Furthermore, the absorption coefficients for walls and floor were set as frequency-independent constants; recalibrating these coefficients to better match the measured reverberation time could bring the simulated T20 closer to the measured reference.

Nevertheless, S-VS was shown to reproduce acoustic properties such as clarity and definition reasonably well. This suggests that applying post-processing to extend the reverberation time could yield reverberation that more closely resembles that of a real acoustic environment, offering a practical path toward perceptually convincing reverberation for virtual spaces.

A natural question for interactive reverberation applications is whether this advantage is maintained when the receiver position is changed. To examine this, measurements were also performed at two additional receiver positions P2 and P3, with offsets of $(0.7, 1.3)$ m and $(1.3, 0.7)$ m from S1, respectively. The positions are shown in Fig. 8.

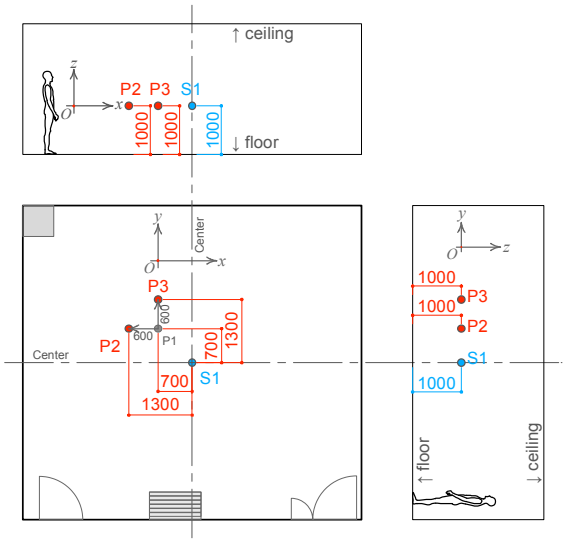



**Fig. 8:** Plan and cross-sectional view of source S1 and receiver positions P2 and P3.

In this evaluation, S-VS at P2 and P3 is obtained by re-estimating the geometric contribution of each VS to the new receiver position, without performing an additional simulation. Specifically, the spatial position of each VS is estimated from its arrival time $\tau_k$ and direction $\hat{\mathbf{d}}_k$ at the reference position $R_0$ as $\mathbf{r}_k = R_0 + c\,\tau_k\,\hat{\mathbf{d}}_k$, where $c$ is the speed of sound. The arrival time, direction, and amplitude are then updated for the new receiver position $R'$ as:

$$\tau'_k = \frac{\|\mathbf{r}_k - R'\|}{c}$$

$$\hat{\mathbf{d}}'_k = \frac{\mathbf{r}_k - R'}{\|\mathbf{r}_k - R'\|}$$

$$I'_k = I_k \cdot \left(\frac{\|\mathbf{r}_k - R_0\|}{\|\mathbf{r}_k - R'\|}\right)^2.$$

This update holds the VS positions fixed and recalculates only the geometric relationships between each VS and the new receiver, enabling S-VS to be applied to P2 and P3 from a single simulation at P1 while GA-IR requires an independent simulation at each position.

Tables 3 and 4 show the averaged room acoustic parameters at P2 and P3. S-VS shows smaller deviations from M-IR than GA-IR across most metrics and frequency

**Table 3:** Room acoustic parameters at P2: M-IR (reference), S-VS, and GA-IR.

| Metric (JND) | Cond. | Freq. band | | | |
|---|---|---|---|---|---|
| | | LF | MF | HF | All |
| T20 (±5%) | M-IR | 0.85 | 1.22 | 1.31 | 1.24 |
| | S-VS | 1.08 | 1.06 | 1.05 | 1.05 |
| | diff. | **+26.0%** | **−13.1%** | **−19.5%** | **−15.3%** |
| | GA-IR | 1.08 | 1.00 | 0.94 | 0.95 |
| | diff. | +26.6% | −18.7% | −27.7% | −22.9% |
| C80 (±1.0 dB) | M-IR | 5.4 | 6.1 | 7.0 | 6.8 |
| | S-VS | 3.6 | 4.1 | 4.5 | 4.5 |
| | diff. | **−1.8** | **−2.0** | **−2.5** | **−2.3** |
| | GA-IR | 12.2 | 12.2 | 11.3 | 11.6 |
| | diff. | +6.8 | +6.1 | +4.3 | +4.8 |
| D50 (±0.05) | M-IR | 0.540 | 0.709 | 0.761 | 0.736 |
| | S-VS | 0.490 | 0.570 | 0.602 | 0.601 |
| | diff. | **−0.049** | **−0.138** | −0.159 | **−0.135** |
| | GA-IR | 0.899 | 0.891 | 0.878 | 0.887 |
| | diff. | +0.360 | +0.183 | **+0.118** | +0.151 |
| Ts (±10.0 ms) | M-IR | 59.4 | 47.7 | 42.8 | 44.3 |
| | S-VS | 71.8 | 61.6 | 58.3 | 58.1 |
| | diff. | **+12.4** | **+14.0** | **+15.5** | **+13.8** |
| | GA-IR | 20.3 | 18.5 | 21.7 | 20.4 |
| | diff. | −39.1 | −29.2 | −21.1 | −23.9 |

**Table 4:** Room acoustic parameters at P3: M-IR (reference), S-VS, and GA-IR.

| Metric (JND) | Cond. | Freq. band | | | |
|---|---|---|---|---|---|
| | | LF | MF | HF | All |
| T20 (±5%) | M-IR | 0.79 | 1.16 | 1.21 | 1.16 |
| | S-VS | 1.18 | 1.10 | 1.06 | 1.07 |
| | diff. | **+48.5%** | **−4.8%** | **−12.3%** | **−7.9%** |
| | GA-IR | 1.18 | 1.01 | 0.94 | 0.95 |
| | diff. | +48.8% | −13.4% | −22.2% | −17.7% |
| C80 (±1.0 dB) | M-IR | 5.3 | 6.0 | 6.9 | 6.7 |
| | S-VS | 4.6 | 4.9 | 4.7 | 4.8 |
| | diff. | **−0.7** | **−1.0** | **−2.2** | **−2.0** |
| | GA-IR | 12.6 | 12.8 | 11.8 | 12.1 |
| | diff. | +7.3 | +6.8 | +4.9 | +5.3 |
| D50 (±0.05) | M-IR | 0.698 | 0.723 | 0.761 | 0.756 |
| | S-VS | 0.561 | 0.622 | 0.621 | 0.622 |
| | diff. | **−0.137** | **−0.101** | −0.141 | **−0.134** |
| | GA-IR | 0.913 | 0.914 | 0.893 | 0.900 |
| | diff. | +0.215 | +0.191 | **+0.131** | +0.144 |
| Ts (±10.0 ms) | M-IR | 46.7 | 47.0 | 42.9 | 42.8 |
| | S-VS | 62.8 | 57.5 | 57.8 | 57.2 |
| | diff. | **+16.1** | **+10.4** | **+14.9** | **+14.4** |
| | GA-IR | 19.7 | 16.6 | 19.9 | 18.7 |
| | diff. | −27.1 | −30.4 | −23.0 | −24.1 |

groups at both positions, consistent with the results at P1. GA-IR again shows notably large deviations particularly for C80, D50, and Ts. These results confirm that the receiver position adaptation maintains the advantage of the wave-based approach over geometrical acoustics.

These results suggest that the proposed framework is capable of generating perceptually realistic reverberation for virtual spaces while supporting receiver position adaptation from a single simulation, indicating strong potential for practical use in interactive reverberation applications.

These findings suggest several directions for future work. Improving simulation accuracy—through more faithful modeling of boundary geometry and recalibration of absorption coefficients to match measured reverberation times—is expected to address the tendency of S-VS to underestimate T20. Alternatively, post-processing to extend the reverberation time of the generated VSVerb could offer a practical near-term solution. The receiver position update could also be extended to handle source position changes, enabling fully flexible 6DoF reverberation rendering for VR and gaming applications. Finally, perceptual evaluation through listening tests would provide a complementary assessment beyond the objective room acoustic parameters examined here.

## 6 Conclusion

This paper presented a framework that extends VSVerb to use pressure and three-axis particle velocity computed by dG-FEM wave-based simulation, enabling 4pi reverberation generation that reflects the acoustic characteristics of virtual spaces.

Experiments in a university lecture room demonstrated that the simulation-based VS distributions and their corresponding impulse responses closely match those derived from actual measurements, confirming that the proposed framework can generate spatially accurate reverberation for virtual acoustic environments. Comparison with measured impulse responses and geometrical acoustics ray tracing showed that the proposed method reproduces room acoustic parameters—such as clarity and definition—closer to the measured reference across most metrics and frequency bands. A tendency to underestimate T20 was observed in S-VS, likely related to simulation accuracy, and post-processing to extend reverberation time is identified as a practical path toward improvement.

Furthermore, receiver position adaptation for 6DoF navigation was demonstrated by re-estimating the geometric contribution of each VS from a single simulation, maintaining the advantage over geometrical acoustics at all evaluated positions. These results indicate that the

proposed framework has clear potential for practical application as a wave-based interactive reverberator for virtual spaces.

## References


[1] Yamasaki, Y. and Itou, T., "Measurement of spatial information in sound field by closely located four point microphone method," *J. Acoust. Soc. Jpn. (E)*, 10, pp. 101–110, 1989.

[2] Sekiguchi, K., Kimura, S., and Hanyu, T., "Analysis of sound field on spatial information using a four-channel microphone system based on regular tetrahedron peak method," *Appl. Acoust.*, 37, pp. 305–323, 1992.

[3] Guy, R. W. and Abdou, A., "A measurement system and method to investigate the directional characteristics of sound fields in enclosures," *Noise Control Eng. J.*, 41, pp. 8–18, 1994.

[4] Nakahara, M., Nagatomo, Y., and Omoto, A., "VSVerb, a practical method of reproducing spatial reverberation from virtual sound sources captured in a room," in *Proc. 24th International Congress on Acoustics (ICA)*, Gyeongju, Korea, 2022.

[5] Yamazaki, J., Nakahara, M., and Nakauchi, S., "Archiving room acoustics of a historic studio by 4pi scene-based sampling reverb, VSVerb," in *Workshop, 155th Convention of the Audio Engineering Society*, New York, 2023.

[6] Hara, R., Nakahara, M., and Omoto, A., "Generating $4\pi$ reverberation using virtual sound sources detected from wave-based simulated responses," in *Proc. 6th Joint Meeting of the Acoustical Society of America and the Acoustical Society of Japan*, Honolulu, USA, 2025.

[7] Nakahara, M., Omoto, A., and Nagatomo, Y., "VSV (Virtual Source Visualizer), a practical tool for 3D-visualizing acoustical properties of spatial sounds," Conv. e-Brief, AES 140th Convention, 2016.

[8] Nakahara, M., Omoto, A., and Nagatomo, Y., "Accurate extraction of dominant reflections from measured sound intensity responses in a room," Conv. e-Brief, AES 142nd Convention, 2017.

[9] Nakahara, M., Nagatomo, Y., and Omoto, A., "Generate $4\pi$ SBA reverberation from virtual sound sources detected from x-y-z sound intensities. —Improvement of the source detection method," Conv. Express Paper, AES 160th Convention, 2026.

[10] Hanyu, T. and Hoshi, K., "Method for analyzing sound pressure and sound particle velocity using cardioid microphones," *Acoust. Sci. & Tech.*, 45(2), 2024.

[11] ISO, "Acoustics—Measurement of room acoustic parameters— Part 1: Performance spaces," ISO Standard 3382-1, International Organization for Standardization, 2009.